Scilight

Thermal Technology and Artificial Intelligence in Health Informatics
https://www.sciltp.com/journals/ttaihi

Case Report

Bedside Monitoring Infrared Thermography in Pediatrics: A Proposed Classification for Complex Wounds in Intensive Care in Uruguay

Sergio Machado [1,2,*,†], Andrea Rodriguez [1,3,†], Vincenzo Rosso, [1,4,†], Romina Alonso [1,†] and Gabriela Iglesias [1,†]

1 Thermology Team Pereira Rossell Hospital, Montevideo 11610, Uruguay
2 Uruguayan Association of Medical Thermology, Buceo, Montevideo 11600, Uruguay
3 Children's Intensive Care Unit, Pereira Rossell Hospital, UDELAR, Montevideo 11600, Uruguay
4 Biochemistry Engineering, Engineering, Faculty of Engineering, Universidad Viña del Mar, Valparaíso 2520000, Chile
* Correspondence: sergioandres2976@hotmail.com
† These authors contributed equally to this work.

How To Cite: Machado, S.; Rodriguez, A.; Rosso, V.; et al. Bedside Monitoring Infrared Thermography in Pediatrics: A Proposed Classification for Complex Wounds in Intensive Care in Uruguay. *Thermal Technology and Artificial Intelligence in Health Informatics* **2025**, *1*(1), 2.

Received: 4 August 2025
Revised: 25 September 2025
Accepted: 12 October 2025
Published: 6 November 2025

Abstract: Wounds in pediatric patients represent a major clinical challenge. Infrared imaging has shown promising diagnostic value because it is a non-invasive non-ionizing radiation method, has fewer adverse effects, does not require sedation and mobilization of critically ill patients. Objective**:** To describe a clinical case in a patient with a post-surgical wound, proposing a possible experimental thermal classification of Thermal Ring (TR) complementary to optical scales for wound and healing measurement. Methods: A 320 × 240-pixel infrared sensor was used. A wound was recorded for 4 weeks and analyzed with specific thermal software. Results: In the first week, the wound bed was observed to be warm, and the TR around the wound was partially formed, with a Tmax of the wound bed of 36.1 °C, corresponding to TR type 1. In the second week, we observed a decrease in the wound bed temperature, with a progressive increase in TR, with a Tmax of the wound bed of 35.6 °C, corresponding to TR type 2. In the third week, there was a decrease in the wound bed temperature, and the edges generated a complete, with a Tmax of 32.1 °C, corresponding to TR 3. In the fourth week, we observed a complete TR, cold bed, with a Tmax of 33.4 °C, corresponding to TR 4. Discussion and Conclusions: This is a case that allowed to describe the thermal behavior of a wound that evolved favorably clinically and could allow to recognize early phenomena that allow future guide health teams regarding expected thermal behavior along with clinical decisions.

Keywords: thermography; wounds; profiles; thermal hyperemia

1. Introduction

The skin is the largest organ in the human body in terms of surface area. It is the fundamental structure that protects internal tissues from mechanical damage, microbial infections, ultraviolet radiation, and extreme temperatures. This makes it highly susceptible to injury, with a significant impact on both patients and the healthcare economy. In the United States alone, non-healing wounds represent approximately $50 billion, scars from surgical incisions and trauma represent nearly $12 billion, and burns account for $7.5 billion in healthcare costs each year [1,2]. Patients with diabetes, the elderly, and patients with genetic disorders, such as sickle cell anemia, are especially predisposed to abnormal wound healing, leading to long-term sequelae.

Chronic and complicated wounds in patients with advanced chronic kidney disease represent a clinical challenge due to their high susceptibility to infection, impaired wound healing, and risk of systemic complications [1]. Skin thermography is a noninvasive tool that allows real-time monitoring of the inflammatory and vascular evolution of lesions, facilitating therapeutic decision-making [2,3]. We present a case illustrating its usefulness in monitoring a post-nephrectomy abscessed wound.

Skin repair requires the intricate synchronization of several cell types in sequential steps. In healthy skin, the epidermis is the outer, impermeable layer that resists the elements. The epidermis also contains the sebaceous glands, sweat glands, and hair follicles [2]. The dermis is rich in extracellular matrix (ECM), vasculature, and mechanoreceptors, and provides the skin with strength, nutrients, and immunity [3,4]. Subcutaneous adipose tissue lies beneath the dermis and functions as an energy reserve. It is also a constant source of growth factors for the dermis. In addition to these cell types, each layer contains resident immune cells that constantly monitor the skin for damage. When the skin is injured, the multiple cell types in these three layers must coordinate in precise steps to achieve healing. These steps of hemostasis, inflammation, angiogenesis, growth, reepithelialization, and remodeling occur in a temporal sequence, but they also overlap [5–7]. Therefore, skin repair is one of the most complex processes in the human body.

Chronic wounds are common in diabetes, vascular diseases, and aging, as well as in patients with hemoglobinopathies. Improper wound care causes recurrences and can lead to limb amputations and mortality. In chronic wounds, the healing process occurs by secondary intention, prolonging the inflammation phase, allowing healing to evolve in its corresponding phases from weeks to months and even years, until spontaneous closure [8–10]. Furthermore, the importance of being able to correlate the phenomena of a wound with its evolutionary time is key to understanding the pathophysiological phenomena that occur in the evolutionary stages of the wound, with the second week determining the beginning of the change in cell type in the three areas of interest in the wound bed, edge, and surrounding area [11–13].

In 2011, the RESVECH 2.0 Index for the Assessment of Chronic Wound Healing was developed to achieve consensus among professionals responsible for the care of patients with chronic wounds [14–17].

This index contains six measurement categories designed to assess the healing process of chronic wounds. Length is recorded cephalocaudal, and width perpendicular to the length (both expressed in cm^2). This is a visual anatomical examination that does not consider metabolic, vascular, and inflammatory phenomena invisible to the human eye [18–21].

Infrared (IR) imaging has the potential to be used as a complementary semiological tool in wounds, given that it is noninvasive, generates no adverse effects, does not require sedation, does not require the mobilization of critically ill patients, and does not generate ionizing radiation [2,5,7]. It can provide qualitative and quantitative information regarding the local evolution of inflammatory processes, and thus monitor responses to different treatments [3,6].

Another important fact is that optical wound measurement using cm^2 scales does not take into account the functional elements of the wound (perfusion, inflammation) [15,17,18]. In this work, we consider the contribution of infrared imaging to wounds, its clinical value, and its ability to understand pathophysiological phenomena at the patient's bedside, considering the metabolic, vascular, and inflammatory aspects of the wound [15,21,22]. Several authors report on the importance of recognizing the phenomenon of Thermal Ring (TR) through thermal profiling (which represents the evolving inflammatory response of wounds, its presence in response to healing phenomena, and the quantification of temperatures along wound sectors, represents the functional phenomena of a wound from a thermal perspective, such as the ring of heat around the wound bed.) [15,21,22]. The use of infrared imaging has increased in the last 20 years. Analysis by thermal sensors produces a high-resolution image called a thermogram [7–10], demonstrating its contribution to diverse applications such as rheumatology, plastic surgery, palliative care, vascular pathology, diabetic foot, neoplasia, cardiology, ICU, occupational medicine, pain therapy, toxicology and sports medicine [18–20]. It has high sensitivity and specificity in providing information on the metabolism, perfusion and inflammation of a region of interest (ROI) [22,23]. For its correct interpretation, knowledge of the pathophysiology, thermodynamics and thermokinetics of human skin is essential [20]. The regulation of skin temperature is a complex system that depends on blood flow, local structures of the subcutaneous tissues, sympathetic nervous system activity, the environment and the individual's basal rate [20].

Objective: Description of a clinical case in a patient with a post-surgical wound, with follow-up using high-resolution thermography at the patient's bedside in a pediatric intensive care unit, proposing in an exploratory manner a thermal classification through the wound thermal ring profile, complementary to optical scales for measuring wounds and healing.

2. Materials and Methods

Infrared images were recorded in the intensive care unit for four weeks. The proposed Pediatric Thermal Wound Protocol (TWP) was used. This protocol consists of exposing the healing wound to thermal equilibrium for 10 min in the room, without performing any procedures during wound opening. The patient was positioned according to the wound location at the level of the posterior lumbar region. The patient’s positioning was performed according to the TWP protocol. The thermal image recording distance was 30 cm using the lumbar window approach of the Uruguayan Association of Medical Thermology. The American Academy of Thermology protocol for point-of-care recording was followed, as well as the Glamorgan protocol. All images were obtained with the signed consent of the patient’s guardians, through a protocol registered with the Ministry of Public Health of Montevideo and approved by the Ethics Committee of the Pediatric Hospital. This work corresponds to a larger project currently being carried out by the research team. The FLIR E75 infrared sensor (IRS) was used. This infrared system has a resolution of 320 × 240 (76,800 pixels), thermal sensitivity/NETD < 0.04 °C/<40 mK, a spectral range of 7.5–14.0 µm, a frame rate of 30 Hz, a field of view (FOV) of 24° × 18° (17 mm lens), and a spatial resolution (IFOV) of 1.31 mrad/pixel. F-number of f/1.3 and continuous focusing. The “rainbow” color scale was used, with the warmest areas in the images represented as white/red, and the cooler areas as blue/black.

Skin emissivity was set at 0.98. The ambient temperature was 24 ± 1 °C. Image acquisition and storage were performed using Vision Fy® Thermal software version 1.2.1. FLIR ResearchIR® software (V 3.0.1) was used to analyze the thermal profiles of the regions of interest (ROIs).

The IRS equipment was blackbody calibrated on 22 May 2020. Images were acquired by a trained thermologist using the aforementioned protocol at distances of 30 cm from the ROIs. No angle tolerance analysis was performed. The emissivity used was that of human skin, as previously mentioned. Ambient airflow was not controlled, and the waiting time after bandage removal was 10 min. A predefined temperature scale was used in the thermograms with an analysis range of 30 °C and 38.5 °C to ensure comparable images from week to week.

The wound thermal profile was calculated from the three areas of interest defined in the ROIs to analyze the thermal distribution pattern over a 4-week period. The areas analyzed through a line crossing over them were defined as: 1-external wound, 2-edge wound, and 3-bed wound. (Figure 1) The temperature variables (Tmax, Tmin, Taverage) of each profile were analyzed. The pixel variable analyzed comprises a distribution of 149 pixels along the profile line, correlated with a 4-week time span. The analysis of the thermal distribution was performed using Python. For each week, descriptive analyses were performed using the Pandas and NumPy libraries, while Matplotlib was used for the graphics.

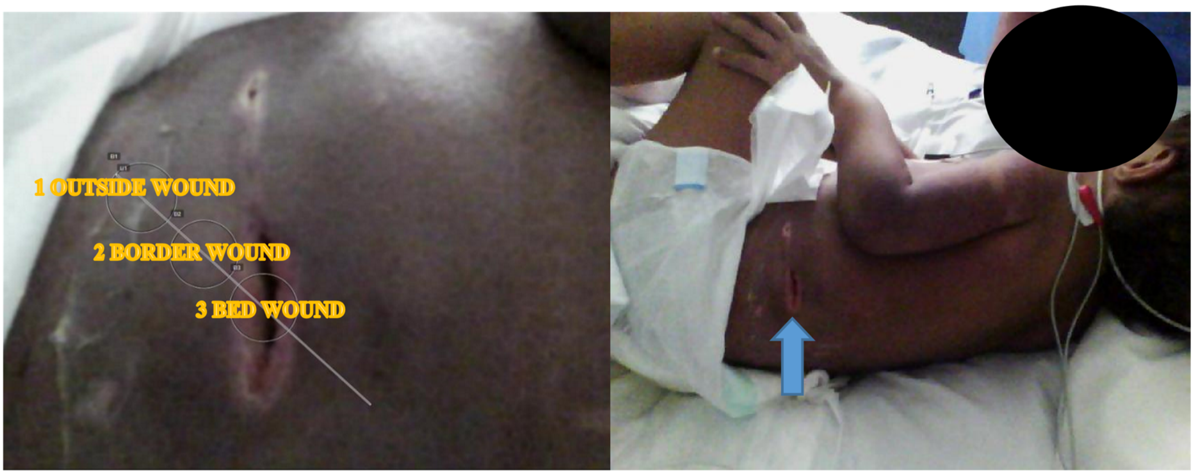

Figure 1. Left: ROI analyzed using the ravé profile. Sectors 1–3, ROI Line, define functional ravés using thermograms. The entire ROI line area, corresponding to 149 pixels, was analyzed. **Right**: ROI studied and patient positioning according to the Thermo Wounds Pediatric protocol.

Case:

A 12-year-old male adolescent with a history of myelomeningocele and hydrocephalus with a ventriculoatrial shunt developed stage 5 chronic kidney disease secondary to obstructive uropathy and neurogenic bladder. He has being undergoing peritoneal dialysis since 2017, with recurrent episodes of peritonitis and sepsis observed during this period.

His main comorbidities included severe arterial hypertension with moderate ventricular failure (LVEF 40%), severe renal osteodystrophy, and secondary hyperparathyroidism (parathyroidectomy in 2023).

Multifactorial anemia with multiple transfusions. In September 2024, he presented with severe nephrourological sepsis due to Klebsiella oxytoca, with a left renal abscess that required nephrectomy and resulted in a wound with a slow-moving abscess. A right nephrectomy was subsequently performed for a refractory hypertensive crisis secondary to renal artery stenosis. Following left nephrectomy, the patient developed an abscessed lesion in the surgical site, with persistent drainage and signs of local infection. The humoral markers are detailed in Table 1, reaching a maximum value of CRP of 110 mg/dL and PCT of 34.5 ng/mL, with leukocytosis values of 18.5 µ/L and axillary temperatures of 37.5 °C under treatment with vancomycin and meropenem. The patient's outcome was unfavorable, requiring multiple dressings, prolonged antibiotic therapy, and a risk of progression to intra-abdominal complications. The wound was monitored by thermography in the intensive care unit for 4 weeks in the intensive care unit.

Table 1. The humoral test values for the referred case.

Values/Records	15 October 2024	22 October 2024	1 November 2024	6 November 2024
Hb g/dL	10	9.2	10.6	10.8
CRP mg/L	80	110	60	40
PCT ng/mL	31.4	34.5	21.6	5.6
Leukocytosis µ/L	14.7	18.5	17.6	11.5
Axillary temp °C	36.1	37.4	37.2	37.2

3. Results

Thermal images for each week are shown in Figures 2–5. The ROI for each image corresponding to each week is shown along with its photographic optical image.

In addition, the thermal behavior related to the pixels of the ROI is recorded. At a qualitative level, the warm wound bed is observed in the first week, and the TR around the wound is partially formed, with a wound bed Tmax of 36.1 °C, corresponding to type 1 TR (Figure 2). In the second week, a clear decrease in wound bed temperature is observed, with a progressive increase in TR around the wound, with a wound bed Tmax of 35.6 °C, corresponding to type 2 TR (Figure 3). In the third week, the decrease in wound bed temperature continues and the edges become harmonized, generating a complete TR, with a Tmax of 32.1 °C, corresponding to type 3 TR (Figure 4). In the fourth week, the complete formation of the TR cold bed was observed, with a Tmax of 33.4 °C, corresponding to TR 4 (Figure 5). Figure 6 shows the ROI distribution over the four weeks.

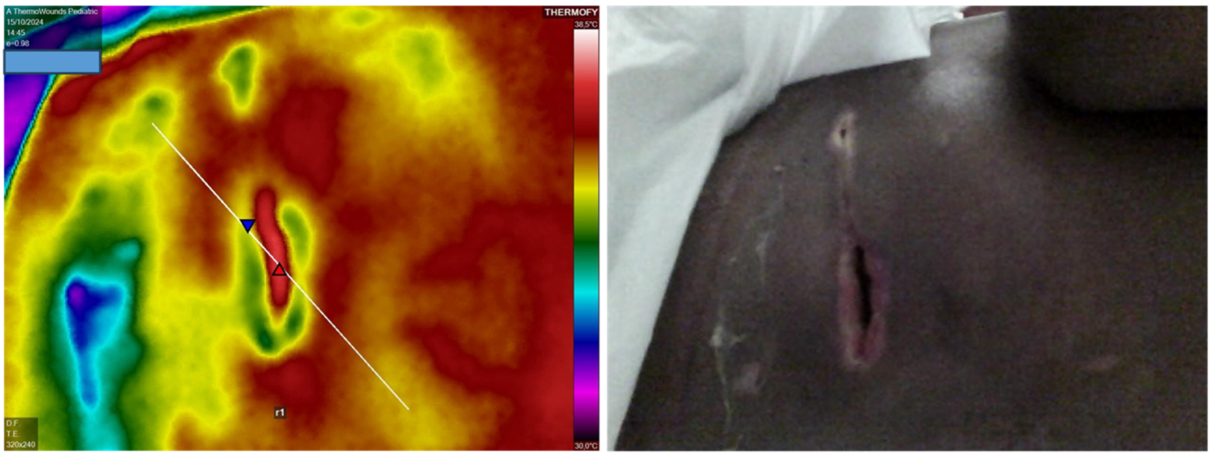

Figure 2. Date:15 October 2024. The hot wound bed is observed in the first week, and the TR around the wound is partially formed, with Tmax of the wound bed 36.1 °C, corresponding to TR type 1. Optical image of the wound to the right.

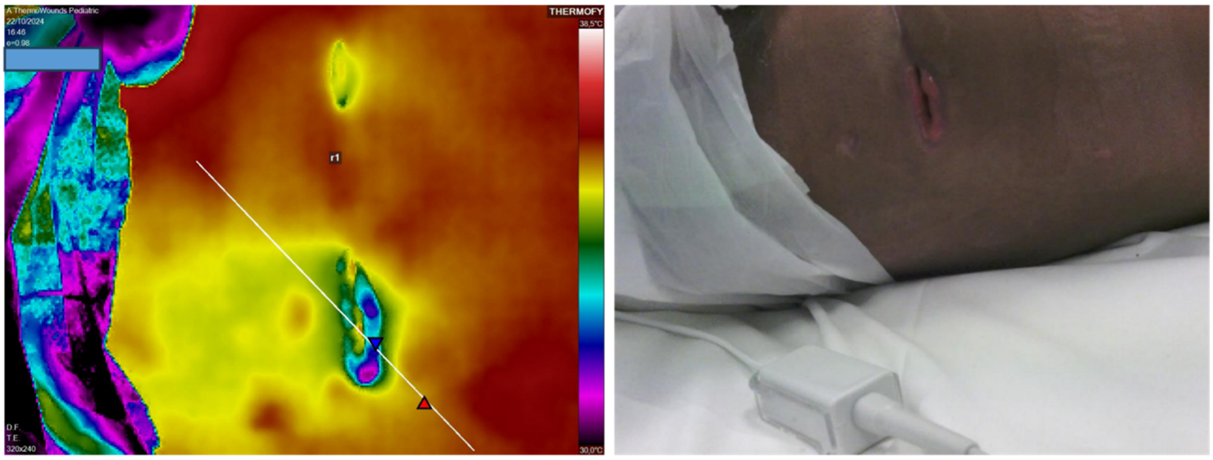

Figure 3. Date: 22 October 2024. In the second week, a clear decrease in the temperature of the wound bed is observed, with a progressive increase in the surrounding TR, with Tmax of the wound bed 35.6 °C, corresponding to TR type 2. Optical image of the wound to the right.

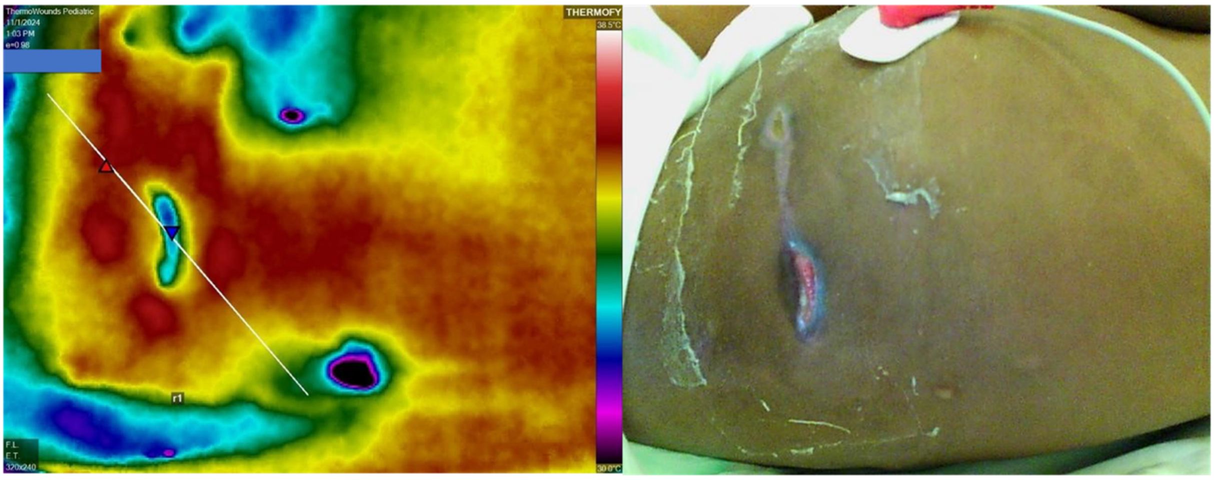

Figure 4. Date: 1 November 2024. In the third week, the temperature of the wound bed continues to decrease, and the edges harmonize, generating a complete TR, with Tmax 32.1 °C. Corresponding to TR type 3. The photograph shows adequate clinical evolution of a dry wound, with vitalized tissue.

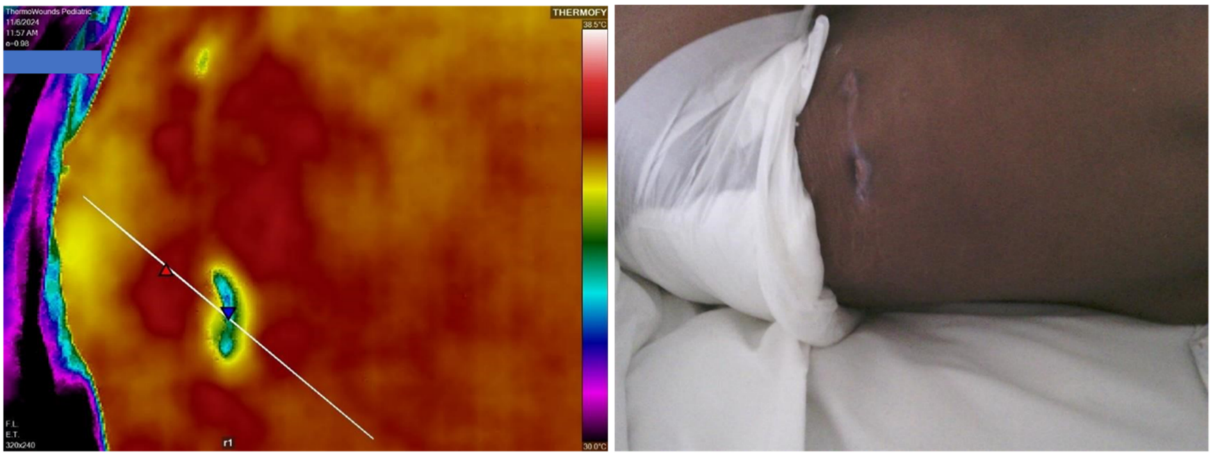

Figure 5. Date: 6 November 2024. In the fourth week we observed the complete conformation of the cold bed TR, with Tmax 33.4 °C, corresponding to type 4 TR. A photograph showing adequate clinical evolution of the dry wound, with vitalized tissue.

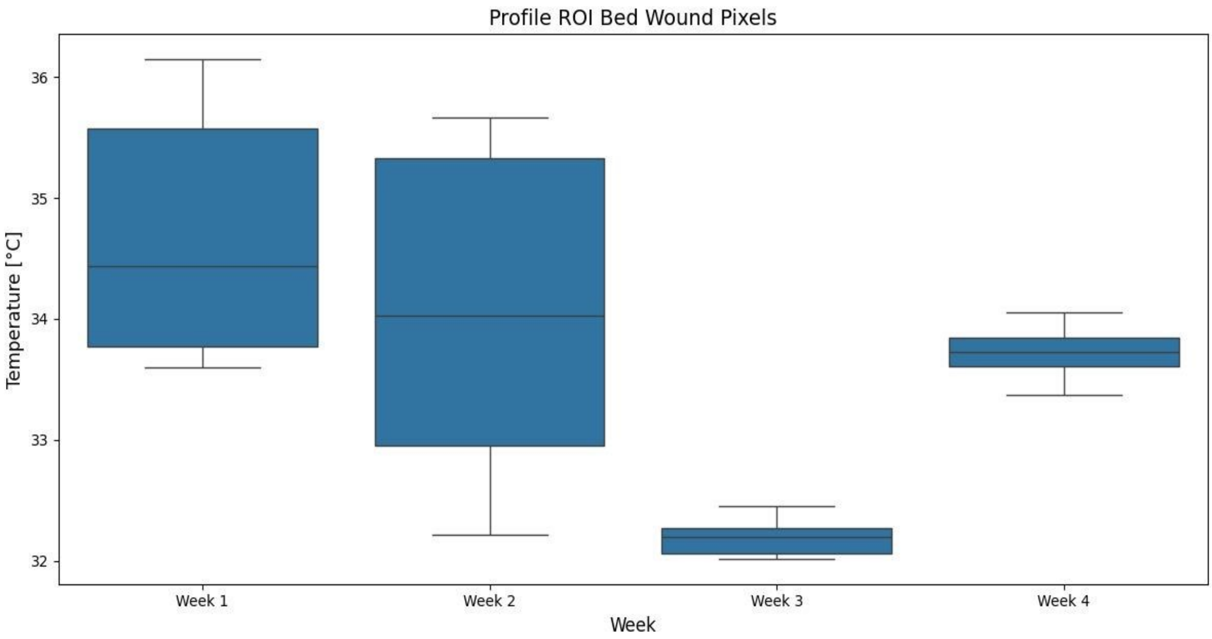

Figure 6. Distribution of evolving temperatures over the wound ROI over the 4 weeks.

The evolutionary record is recorded in the 3D graph (Figure 7), demonstrating the descending pattern of the wound bed and the increasing thermal pattern of the TR.

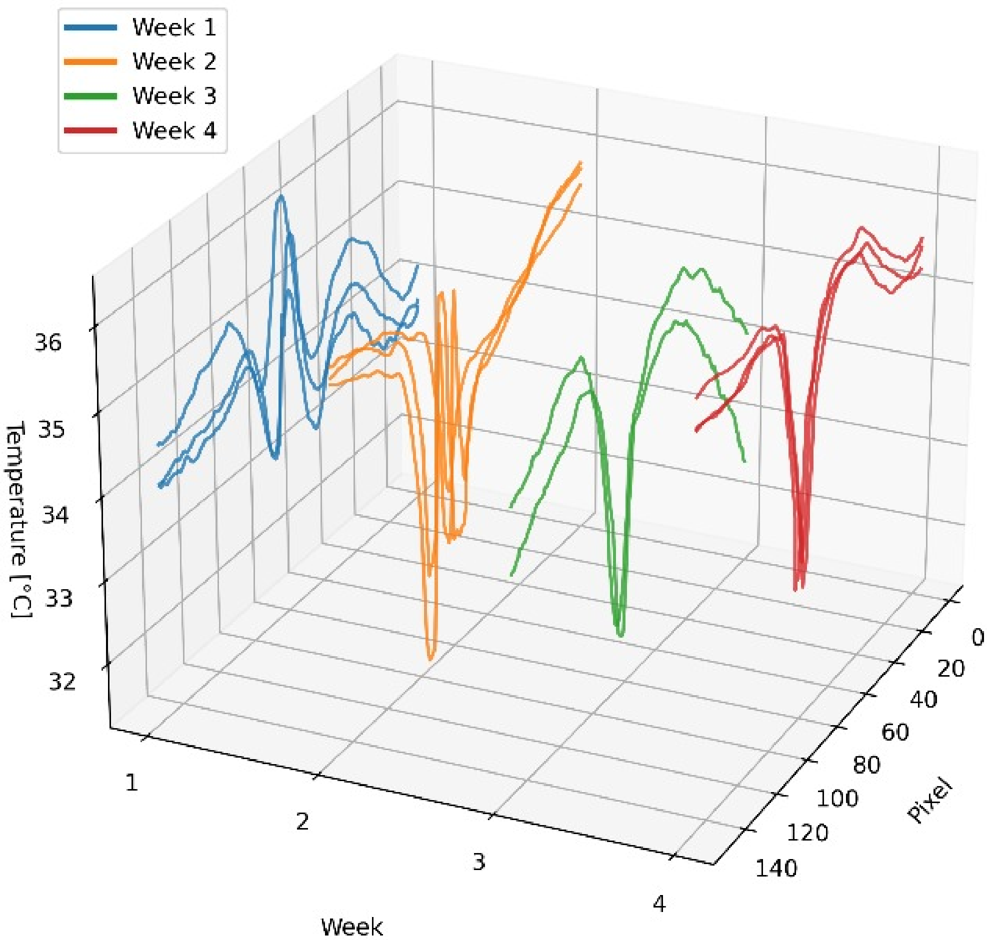

Figure 7. Evolutionary distribution over the 4 weeks of the thermal profile of the TR and Bed.

The bed descends steadily between weeks 1 and 3, reaching its minimum at week 3. From week 4 onwards, an increase in the thermal border (area 2) is observed.

This suggests the possibility of extracting information from the thermal trend of the profile. To this end, we propose a thermal index that allows staging the thermal healing process, along with the classification proposed by the research team.

To this end, the following formula has been proposed to define the index, where 33.5 [°C] represents the average temperature range in the wound in the present case.

To this end, an exploratory descriptive statistical analysis of the profiles for each week was performed, as shown in Table 2.

$$Tw = \frac{\bar{T}_s}{33.5\ [°C]}$$

Tw: wound temperature index.

(T_S): Average wound temperature.

Table 2. TW index per week and its standard deviation.

Week	Average Index	Standard Deviation
1	1.024	0.012
2	1.044	0.006
3	1.029	0.013
4	1.067	0.004

The above allows us to obtain the following results from the profiles.

Figure 8 shows potential differences in the distribution of TW, as well as in the mean and median. This will, therefore, justify an exploratory analysis with a larger number of cases, allowing for an inferential analysis and statistical conclusions that can be extrapolated to the use of the TW Index for pediatric wounds.

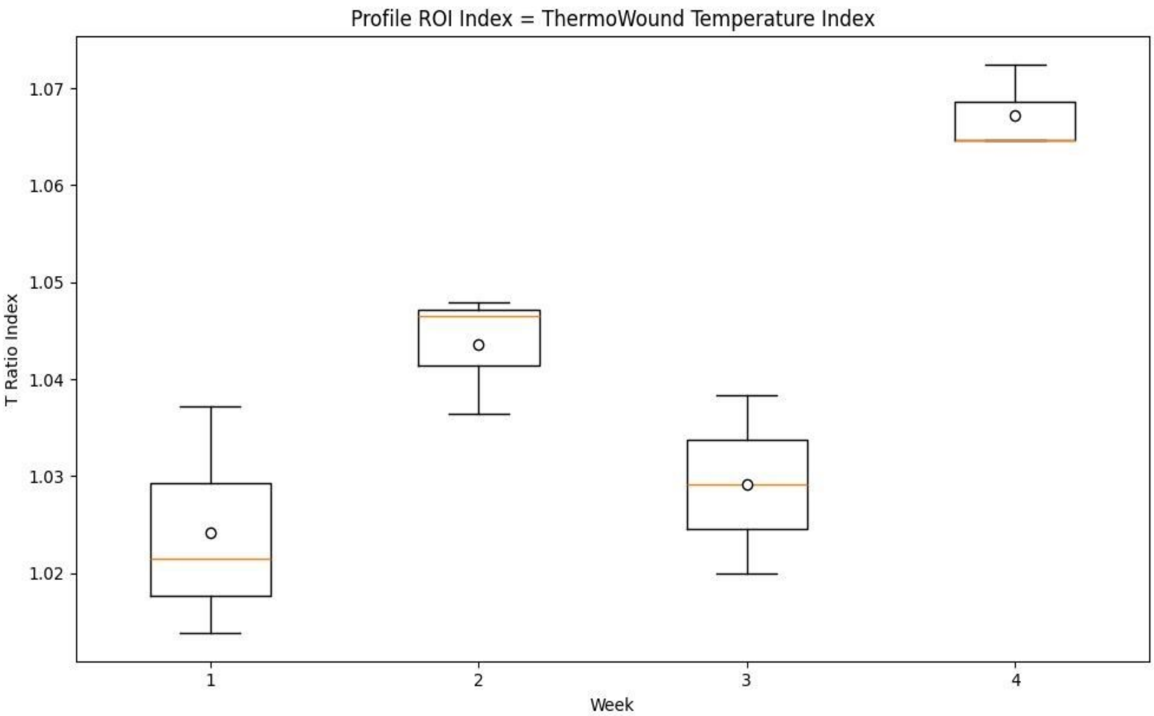

Figure 8. Profile ROI Index. TW Index and its weekly distribution in this case.

4. Discussion

This case, in its evolution, illustrates the possible metabolic, inflammatory, and perfusion behavior of a wound that is clinically progressing favorably toward healing [18,19]. Thermal images show a difference between the functional wound size and the optical size, which could propose the acronym TR as a possible clinical sign in thermal wounds. This TR could be qualitatively linked to the chronology of wound evolution, thus linking it to the healing process. Importantly, with studies with a larger number of cases, the Thermo Wounds Pediatric protocol would offer a fast, clear, and practical way to complement point-of-care wound analysis, along with traditional wound measurement systems such as RESVECH 2.0 and T.I.M.E.R.S [21,22]. These findings are consistent with reports on infectious processes of central venous catheters, with Tmax values exceeding 37.5 °C in inflammatory processes and exceeding 38.6 °C in cases of insertion site infection confirmed by humoral paraclinical tests and catheter culture [14]. Tmax values of 37 °C are also described for venous catheters in cases of suspected infection [15,18]. In their review of thermal patterns in wounds, they reported that average wound temperature patterns were observed in 47% of the studies and maximum temperatures in 26% of the studies [20,23]. Values of 38.8 °C on the first day of wound evolution and 40.2 °C on the seventh day were described [14,16]. They used a cutoff value of 34 °C to predict infectious processes. In this case, the wound presented values similar to those of the wound bed reported by Machado et al. (2025). These values are also similar to those obtained by Childs (2019) in their beds, with values below 33 °C [20,24]. In our case, the perilesional temperature was comparable to that described by Derwin et al. (2022), which was 34 °C. Regarding the recordings and periods of image acquisition, the different authors obtained thermal recordings during the first and second weeks (Derwin et al., 2022), from the first to the seventh day, and subsequently once a week until day 49, from the first to the seventh day [25–27]. Our report was carried out over 4 weeks, and all images were obtained by a specialist in medical thermology, along with the team of physicians and nurses from pediatric intensive care specializing in the bedside monitoring of pediatric wounds [16,24,28].

5. Conclusions

Chronic and infected wounds in patients with CKD and multiple comorbidities are associated with high morbidity and mortality [14]. Factors such as anemia, osteodystrophy, relative immunosuppression, and vascular alterations impair healing and predispose to infectious recurrence [16,18]. Qualitative and quantitative information obtained at the point of care through thermography using the Pediatric Thermo Wounds protocol could complement the clinical evaluation and facilitate decisions such as progressive reduction in wound dressing frequency and gradual discontinuation of antibiotics, based on objective findings.

We propose the possible use of the experimental Thermal Index TW, a product of the hypothetical analyses obtained that could demonstrate potential findings in the interpretation of the evolutionary data. However, further statistical analysis is required to obtain extrapolable data [15–17]. Possible proposal to be used for qualitative thermal TR curves of the wound bed, TW index, qualitative TR pattern and description of wound temperatures through the Profile in clinical wounds [15–18]. (Requires further statistical analysis in the future, see Appendix A).

At one month of follow-up, the wound presented complete resolution with clinically satisfactory healing, with no new local infectious complications [17]. This case highlights the importance of using infrared thermography imaging as a noninvasive monitoring tool for complex wounds in pediatric patients. Given that there is currently no reliable means for interpreting inflammation at the bedside, the incorporation of this tool in intensive care units is warranted [14,15,20].

Although the results suggest a possible disparity between weeks 1 and 4, which may be related to cellular changes during healing, the small sample size and one clinical case do not allow extrapolation, requiring a larger number of clinical cases. This signal, still insufficient to draw definitive conclusions, reinforces the importance of continuing to study the Thermo Wounds Pediatric TR protocol at the point of care [14,16,22].

The research team continues to monitor the wounds, increasing the number of cases, to study the potential statistical significance of these data. The current case allowed us to characterize the thermal behavior of a wound that showed favorable clinical evolution, enabling us to recognize early features that can be used by health teams to predict future thermal behavior and make appropriate clinical decisions.

6. Study Limitations

This study corresponds to a single case, and it is not possible to extrapolate the exploratory results. Not all evolutionary data from the patient's clinical blood tests could be obtained. Infrared images were obtained by a trained thermologist, but the image registration angles could not be protocolized, which may require a stricter protocol. The same thermologist performed the post-processing of the thermograms, adding a potential ROI selection bias that requires exploratory analysis in the team's future research. The recommendation to use the profile scale through the Thermo Wounds Pediatric protocol with profiles to describe TR requires validation, which is currently being studied by the research team with the collection of case series. The lack of calibration of the IRS sensor prior to recording thermal images may limit the accuracy of temperature range measurements. Another element is that measurements were not taken with RESVECH 2.0 scales during data collection; this would have provided optical measurement data, which could have been supplemented with infrared images. The use of bedside thermography is being protocolized, along with measurement scales implemented in the use of T.I.M.E.R.S. in wounds, where we believe the contribution of thermography can be valuable.

Author Contributions

S.M.: conceptualization, methodology, software; A.R.: data curation, drafting of the original version; V.R.: visualization, descriptive statistics; R.A.: writing; G.I.: bibliographic references. All authors have read and approved the published version of the manuscript.

Funding

This research received no external funding.

Institutional Review Board Statement

The ethics committee of the Pereira Rossell Hospital Center approved the conduct of this research.

Informed Consent Statement

The clinical case presented has the endorsement and consent signed by the patient's guardian.

Data Availability Statement

We advocate for the sharing of research data by all authors contributing to publications in Scilight journals. In this section, authors may be asked to provide the raw data of their study together with the manuscript for editorial review and should be prepared to make the data publicly available if practicable. In any event, authors should ensure accessibility of such data to other competent professionals for at least 10 years after publication (preferably via an institutional or subject-based data repository or other data center), provided that the confidentiality of the participants can be protected and legal rights concerning proprietary data do not preclude their release. In instances where novel data were not generated or data remains inaccessible due to privacy or ethical considerations, a clear statement outlining these circumstances is mandatory.

Acknowledgments

We would like to thank the Pediatric Intensive Care Unit team at Pereria Rossell Hospital for the opportunity to work with a multidisciplinary team.

Conflicts of Interest

The authors declare no conflict of interest.

Use of AI and AI-Assisted Technologies

No AI tools were utilized for this paper.

Appendix A. Qualitative Thermal TR Curves of the Wound Bed, TW Index, TR Pattern and Wound Bed Tmax Table

Thermo Wounds Pediatric	Thermal Ring	Wound Bed	Week	Índice TW	TR Pattern	Wound Bed Tmax
Type 1	Partial Ring	Hot	1	1.03	Profile absent	36–35 °C
Type 2	Partial Ring	Cold	2	1.05	Profile present	35–34 °C
Type 3	Full Ring	Cold	3	1.03	Profile present	34–33 °C
Type 4	Full Ring	Cold	4	1.07	Profile present	33–32 °C

Appendix B. Raw Thermal Image IRS and Profile Selection

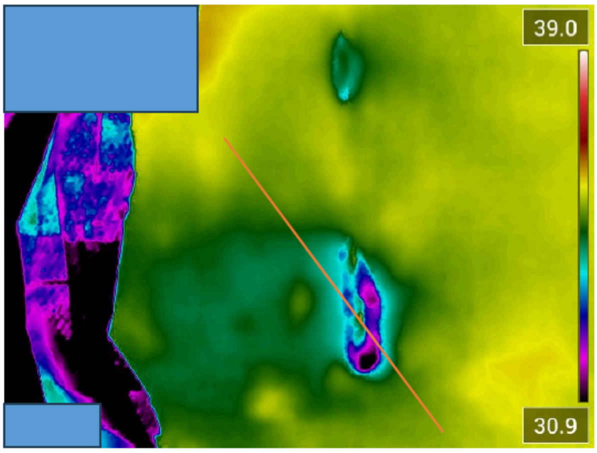

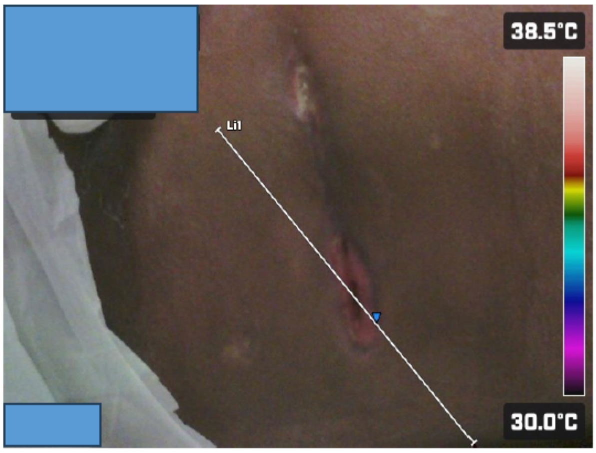

References

1. Power, G.; Moore, Z.; O'Connor, T. Measurement of pH, exudate composition and temperature in wound healing: A systematic review. *J. Wound Care* **2017**, *26*, 381–397.
2. Kanazawa, T.; Kitamura, A.; Nakagami, G.; et al. Lower temperature at the wound edge detected by thermography predicts undermining development in pressure ulcers: A pilot study. *Int. Wound J.* **2016**, *13*, 454–460.
3. Alsaaod, M.; Schaefer, A.L.; Büscher, W.; et al. The role of infrared thermography as a non-invasive tool for the detection of lameness in cattle. *Sensors* **2015**, *15*, 14513–14525.
4. Childs, C.; Soltani, H. Abdominal cutaneous thermography and perfusion mapping after caesarean section: A scoping review. *Int. J. Environ. Res. Public. Health* **2020**, *17*, 8693.
5. Monshipouri, M.; Aliahmad, B.; Ogrin, R.; et al. Thermal imaging potential and limitations to predict healing of venous leg ulcers. *Sci. Rep.* **2021**, *11*, 13239.
6. Zhu, L.Y.; Guo, S.X.; Wu, P.; et al. Advances in the research of the relationship between wound temperature and wound healing. *Zhonghua Shao Shang Za Zhi Zhonghua Shaoshang Zazhi Chin. J. Burns* **2018**, *34*, 829–832.
7. Schollemann, F.; Kunczik, J.; Dohmeier, H.; et al. Infection probability index: Implementation of an automated chronic wound infection marker. *J. Clin. Med.* **2022**, *11*, 169. https://doi.org/10.3390/jcm11010169.
8. McKinney, W. *Python for Data Analysis: Data Wrangling with Pandas, NumPy, and IPython*, 2nd ed.; O'Reilly: Springfield, MI, USA, 2017.
9. Harris, C.R.; Millman, K.J.; van der Walt, S.J.; et al. Array programming with NumPy. *Nature* **2020**, *585*, 357–362.
10. Hunter, J.D. Matplotlib: A 2D graphics environment. *Comput. Sci. Eng.* **2007**, *9*, 90–95.
11. Virtanen, P.; Gommers, R.; Oliphant, T.E.; et al. SciPy 1.0: Fundamental Algorithms for Scientific Computing in Python. *Nat. Methods* **2020**, *17*, 261–272. https://doi.org/10.1038/s41592-019-0686-2.
12. Li, F.; Wang, M.; Wang, T.; et al. Smartphonebased infrared thermography to assess progress in thoracic surgical incision healing: A preliminary study. *Int. Wound J.* **2023**, *20*, 2000–2009. https://doi.org/10.1111/iwj.14063.
13. Ramirez, J.; Bartlett, R.; Arriaga, J.; et al. Infrared thermography in wound care, surgery, and sports medicine: A review. *Front. Physiol.* **2022**, *13*, 838528. https://doi.org/10.3389/fphys.2022.838528.
14. Machado, S.; Rodríguez, A.; Guerrero, J.; et al. Termografía infrarroja de alta resolución para monitoreo de catéteres venosos centrales en una unidad de cuidados intensivos pediátricos en Uruguay. *Arch. Pediatría Urug.* **2025**, *96*, e301. https://doi.org/10.31134/ap.96.5.
15. Fridberg, M.; Rahbek, O.; Husum, H.-C.; et al. Can pin-site inflammation be detected with thermographic imaging? A cross-sectional study from the USA and Denmark of patients treated with external fixators. *Acta Orthop.* **2024**, *95*, 562–569. https://doi.org/10.2340/17453674.2024.41901.
16. Fridberg, M. *Postoperative Infection Monitoring Using Thermography*; Aalborg University Open Publishing: Aalborg Øst, Denmark, 2025; 140p.
17. Childs, C.; Wright, N.; Willmott, J.; et al. The surgical wound in infrared: Thermographic profiles and early stage test-accuracy to predict surgical site infection in obese women during the first 30 days after caesarean section. *Antimicrob. Resist. Infect. Control* **2019**, *8*, 1–15. https://doi.org/10.1186/ s13756-018-0461-7.
18. Burke-Smith, A.; Collier, J.; Jones, I. A comparison of non-invasive imaging modalities: Infrared thermography, spectrophotometric intracutaneous analysis and laser Doppler imaging for the assessment of adult burns. *Burns* **2015**, *41*, 1695–1707. https://doi.org/10.1016/j.burns.2015.06.023.

19. Mercer, J.B.; Nielsen, S.P.; Hoffmann, G. Improvement of wound healing by water-filtered infrared-A (wIRA) in patients with chronic venous stasis ulcers of the lower legs including evaluation using infrared thermography. *Ger. Med. Sci.* **2008**, *6*, Doc11.
20. Machado, S.; Tortorella, M.; Medeiros, C.; et al. Uso da imagem infravermelha em caso de envenenamento de uma criança picada por Bothrops Pubescens (Cope, 1870) no Uruguay. *Pan Am. J. Med. Thermol.* **2023**, *10*, e2023005. https://doi.org/10.18073/pajmt.2023.10.005.
21. Dang, J.; Lin, M.; Tan, C.; et al. Use of infrared thermography for assessment of burn depth and healing potential: A systematic review. *J. Burn. Care Res.* **2021**, *42*, 1120–1127. https://doi.org/10.1093/jbcr/irab108.
22. Carriere, M.E.; Haas, L.E.M.; Pijpe, A.; et al. Validity of thermography for measuring burn wound healing potential. *Wound Repair. Regen.* **2020**, *28*, 347–354. https://doi.org/10.1111/wrr.12786.
23. Singer, A.J.; Relan, P.; Beto, L.; et al. Infrared thermal imaging has the potential to reduce unnecessary surgery and delays to necessary surgery in burn patients. *J. Burn. Care Res.* **2016**, *37*, 350–355. https://doi.org/10.1097/BCR.0000000000000330.
24. Martínez-Jimenez, M.A.; Ramirez-GarciaLuna, J.L.; Kolosovas-Machuca, E.S.; et al. Development and validation of an algorithm to predict the treatment modality of burn wounds using thermographic scans: Prospective cohort study. *PLoS ONE* **2018**, *13*, e0206477.
25. Bharara, M.; Schoess, J.; Nouvong, A.; et al. Wound inflammatory index: A “proof of concept” study to assess wound healing trajectory. *J. Diabetes Sci. Technol.* **2010**, *4*, 773–779. https://doi.org/10.1177/193229681000400402.
26. Senneville, E.; Lipsky, B.A.; Abbas, Z.G.; et al. Diagnosis of infection in the foot in diabetes: A systematic review. *Diabetes Metab. Res. Rev.* **2020**, *36*, 32176440. https://doi.org/10.1002/dmrr.3281.
27. Derwin, R.; Patton, D.; Avsar, P.; et al. The impact of topical agents and dressing on pH and temperature on wound healing: A systematic, narrative review. *Int. Wound J.* **2022**, *19*, 1397–1408. https://doi.org/10.1111/iwj.13733.
28. Gatt, A.; Falzon, O.; Cassar, K.; et al. The application of medical thermography to discriminate neuroischemic toe ulceration in the diabetic foot. *Int. J. Low. Extremi Wounds* **2018**, *17*, 102–105. https://doi.org/10.1177/ 1534734618783910.